Structural Engineering and Mechanics, *Vol. 59, No. 2 (2016) 209-226*
DOI: http://dx.doi.org/10.12989/sem.2016.59.2.209

Retrofitting of steel pile-abutment connections of integral bridges using CFRP

Seyed Saeed Mirrezaei[a], Majid Barghian[*], Hossein Ghaffarzadeh[b] and Masood Farzam[c]

Department of Civil Engineering, University of Tabriz, 29 Bahman Blvd., Tabriz, Iran

(Received December 21, 2015, Revised March 1, 2016, Accepted March 15, 2016)

Abstract. Integral bridges are typically designed with flexible foundations that include one row of piles. The construction of integral bridges solves difficulties due to the maintenance of expansion joints and bearings during serviceability. It causes integral bridges to become more economic comparing with conventional bridges. Research has been focused not only to enhance the seismic performance of newly designed bridges, but also to develop retrofit strategies for existing ones. The local performance of the pile to abutment connection will have a major effect on the performance of the structure and the embedment length of pile inside the abutment has a key role to provide shear and flexural resistance of pile-abutment connections. In this paper, a simple method was developed to estimate the initial value of embedment length of the pile for retrofitting of specimens. Four specimens of pile-abutment connections were constructed with different embedment lengths of pile inside the abutment to evaluate their performances. The results of the experimentation in conjunction with numerical and analytical studies showed that retrofitting pile-abutment connections with CFRP wraps increased the strength of the connection up to 86%. Also, designed connections with the proposed method had sufficient resistance against lateral load.

Keywords: integral bridge; steel pile-abutment connection; flexural strength of steel pile; embedment length of pile; retrofitting; CFRP

1. Introduction

Integral bridges have many advantages over regular bridges, including lower initial and maintenance costs, reduced noise during vehicle passage, and increased redundancy because of the integral connection between the superstructure and the substructure. In integral bridges, the superstructure is integral with the substructure at the abutment level; consequently, deformations in the superstructure are directly transferred to the substructure. The design of the substructure, specifically the piles, is of great importance and must take into consideration the soil-structure interaction. The complexity of the static and dynamic soil-structure interaction in jointless bridges

*Corresponding author, Ph.D., E-mail: barghian@tabrizu.ac.ir
[a]Ph.D. Student, E-mail: saeed_mirrezaei@tabrizu.ac.ir
[b]Ph.D., E-mail: ghaffar@tabrizu.ac.ir
[c]Ph.D., E-mail: mafarzam@tabrizu.ac.ir

http://www.techno-press.org/?journal=sem&subpage=8 ISSN: 1225-4568 (Print), 1598-6217 (Online)

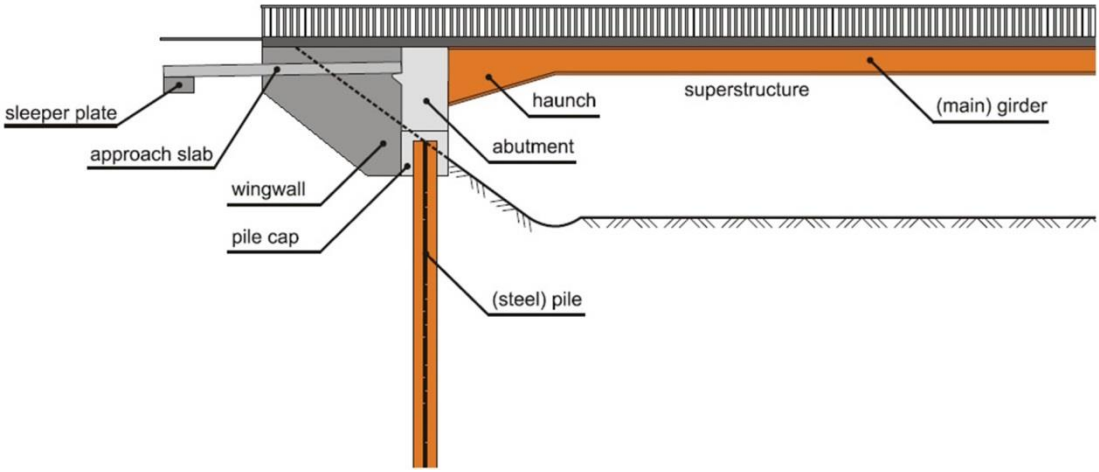

Fig. 1 An integral bridge and its components (Nilsson *et al*. 2008)

requires a limit for the length of jointless bridges. Surveys have shown that this limit is not uniform among agencies and is generally based on a trial-and-error approach (Haj-Najib 2002, Kunin and Alampalli 1999).

To reduce the induced loads from the substructure to the superstructure, flexible foundations, which consist of one row of piles to accommodate longitudinal movements and provide maximum flexibility, are typically recommended (Burke 2009).

A typical integral abutment bridge is shown in Fig. 1. Normally the integral abutment bridge utilizes a single-row of H-piles with bending about their weak axis. However, single row *H* piles with bending about their strong axis and various other pile types (*X* piles, circular concrete piles, steel-concrete composite piles, etc.) with single row or multi rows have also been used (Report 2007, Arsoy 2000 and Petursson 2002). Fig. 2 shows different types of pile-pile cap configurations. In the case of integral bridges, most of the researches have been focused on the effect of static and dynamic soil-abutment interaction in bridge design (Dicleli 2003, 2004, Park 2000, 2001, 2007, Kotsoglou 2009) and only a few articles have been published about the performance of pile to abutment connections and retrofitting of pile to abutment connections (Pam1990, Harries 2001, Xiao 2003, Shama 2001).

Burdette *et al*. (1983) studied concrete bearing strength due to the pressure of rather large steel members embedment inside concrete. In their eight separate tests, large steel members were embedment inside concrete foundation and subjected to lateral forces. Tests results showed that the inserted steel members rotated as a rigid body inside the concrete cap. Also, the results indicated that the average bearing stress on the concrete under failure load was 3.78 f'_c.

Steunenberg *et al*. (1998) performed lateral cyclic load tests on a 12 steel pipe pile with a 0.5 inch wall thickness which was welded to a 25×24 inch×2 inch thick steel plate. The steel plate was attached to the base of a reinforced concrete pile cap using 30 deformed studs, each 0.59 inches in diameter and 23.6 inches long. The moment capacity of the connection exceeded that of the pipe pile and the pile failed in a ductile manner.

Stephens *et al*. (2005) carried out tests on five steel pipe piles filled with concrete with an embedment length of 9 inches inside concrete pile caps. The results of tests showed that using reinforcing steel - in the pile cap - increased the moment capacity of the connection.

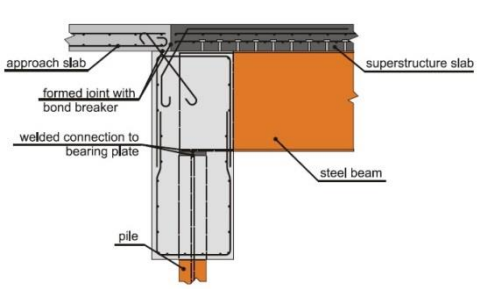

(a) Fixed connection (Nilsson *et al*. 2008)

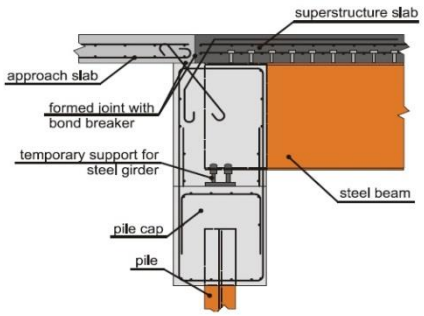

(b) Fixed connection (Nilsson *et al*. 2008)

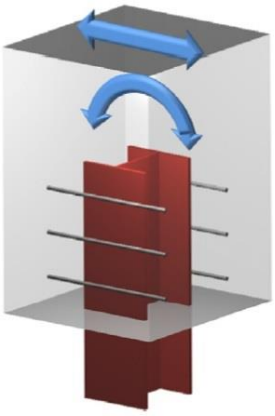

(c) Fixed connection (Ahn *et al*. 2011)

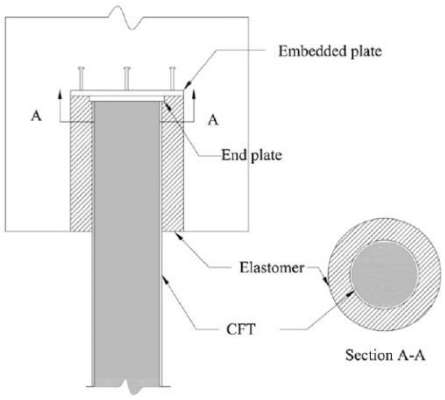

(d) Pinned connection (Sherafati *et al*. 2014)

Fig. 2 Different types of steel pile to abutment connections

Shama *et al*. (2001) found the inflection point of the pile under lateral loads based on analytical study. Two specimens of the connections were subjected to cyclic and lateral loadings. As a retrofit strategy, the effect of increasing of embedment length of pile into foundation was proposed and then by experimental study, the moment capacity of the retrofitted connections was evaluated. The emphasis of this study was on connections where the embedment length of the pile inside concrete was long enough.

Xiao *et al*. (2006) fabricated five full-scale connection specimens and subjected them to lateral and axial cyclic loadings. The study emphasized connections for which the embedment length of the pile inside concrete pile cap was small. The results of tests indicated that although the connection was considered as a pinned connection, it displayed unexpected moment resistance.

Ahn *et al*. (2011) designed five full-scale specimens according to Korean integral bridge design guidelines and subjected them to a static load. To determine the embedment length of the specimens, the effects of shear was neglected and only the effects of bending moments were considered. It was found out that, although the proposed connections with stud shear connectors increased connection resistance, they resulted in a significant ductility decrease of the connection.

Kappes *et al*. (2012) tested 9 half-scale specimens under static loading. The piles were concrete filled steel tubes (CFT). As a result of this research, a new reinforcing scheme was developed that greatly simplified the design and construction of the connection. The newly developed reinforcing scheme included U-shaped reinforcing bars that encircled the embedment CFT piles. The

comparison of force-displacement curves for the connections of the proposed reinforcing scheme with those of conventional reinforcing schemes showed that the proposed connections had higher moment resistance.

Sherafati *et al*. (2014) proposed a flexible connection detail for a steel pile to concrete abutment connection of integral bridges. The preliminary results of the study revealed that a pinned connection - between pile and pile cap - drastically decreased the lateral stiffness of the integral bridge. As a result, the lateral displacement capacity of the bridge was increased, leading to the construction of integral bridges with longer spans possible. The results of the research indicated that the proposed pinned connection was more flexible than the corresponding fixed connection.

As a result of the disastrous consequences of recent earthquakes, some researches have been focused on not only enhancing the seismic performance of newly designed structures, but also to develop retrofit strategies for existing ones. Pile-to-cap connections may exhibit plastic hinging during earthquakes. In such a case, the local performance of the connection will have a major effect on the overall performance of the structure.

FRP (Fiber-reinforced polymers) materials are lightweight, noncorrosive, and exhibit high tensile strength. Although FRP materials are relatively expensive compared with traditional reinforcing materials, the labour and equipment costs to install FRP systems are often lower. FRP systems can also be used in areas with limited access where traditional techniques would be difficult to implement. In the case of integral bridges, access to the pile-abutment connection, using traditional retrofitting methods is difficult. Therefore, retrofitting with FRP can have many advantages.

Reviewing the previous research on steel pile to abutment connections demonstrates a lack of research about retrofitting of steel pile to abutment connections.

The main objective of this research is to evaluate the efficiency of FRP system in retrofitting of steel pile to abutment connections for integral bridges. Therefore, first, a simple method was developed to calculate the required embedment length of the pile, based on the plastic moment of the steel pile. Then, four specimens of pile-abutment connections were constructed with different embedment lengths of pile inside the abutment to evaluate their performance. Two specimens were retrofitted with different details and loading tests were applied to evaluate their structural behaviour.

2. Conventional method of designing steel H-Pile to concrete abutment connection in integral bridges

To predict the behaviour of structures under lateral loads, it is important to determine the locations where plastic hinge formation may occur. In integral bridges, it is important for any possible failures in pile-to-abutment connection to occur in pile and the failure mode must be flexural. Hence, the main purpose of the design criteria is to ensure the connection strength is beyond the plastic flexural strength of steel pile section. Due to the lateral movement of the deck- which is generally caused by earthquakes, daily or annual temperature changes- the superstructure tends to move towards the backfill. This movement subjects the connections to undergo bending moments and shear forces. In the conventional method of designing these types of connections, the shear force is neglected in comparison to the bending moment. As shown in Fig. 3, by eliminating the effects of the shear force, the assumed concrete forces resisting the moment will be of equal magnitude (Ahn *et al*. 2011).

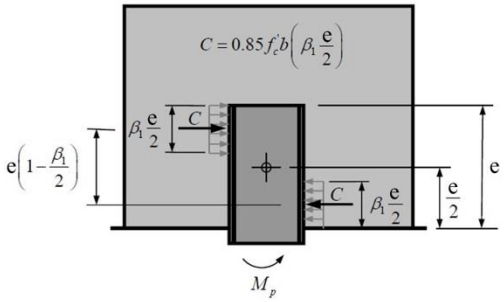

Fig. 3 Rectangular stress distribution around the pile

$$C = 0.85 \times f_c^{/} \times \mathrm{a} \times b_w \tag{1}$$

In Eq. (1), a, is the depth of the equivalent rectangular stress block applied to the pile and, b_w is the width of steel pile section. The equation can be written as (Ahn *et al*. 2011)

$$C = 0.85 \times f_c^{/} \times b_w \times (\beta_1 \times \frac{e}{2}) \tag{2}$$

In this equation, β_1 is the factor relating depth of equivalent rectangular compressive stress block to depth of neutral axis which is defined from section 22.2.2.4.3 of ACI 318-14. According to this section, β_1 is defined based on concrete compressive strength, and is adopted between 0.65 and 0.85.

The embedment length of the pile, *e*, inside abutment is determined by Eq. (3) (*et al*. 2011).

$$e = \sqrt{\frac{2M_P}{0.85 f_c^{/} b_w \beta_1 (1 - \frac{\beta_1}{2})}} \tag{3}$$

Given the flexural strength of the steel pile, defined as the plastic moment, M_p, the specified strength of concrete and the width of the pile cross-section about the bending axis (equal to pile flange width if the bending occurs about the strong axis), the embedment length can be determined by using the Eq. (3).

3. Theoretical model of steel H-pile to concrete abutment connection

The conventional design method summarized by Eq. (3) neglects the effects of the shear force and the design of the connection only accounts for the plastic flexural strength of the pile. In the equations presented in this study, the following assumptions have been made:

- The effect of axial force of the pile on the strength of connection is neglected.
- The combined effect of bending and shear is considered in determining the embedment length of pile inside the concrete abutment.
- The distribution of bearing stress on the plane between the steel pile and concrete abutment is considered to be linear.

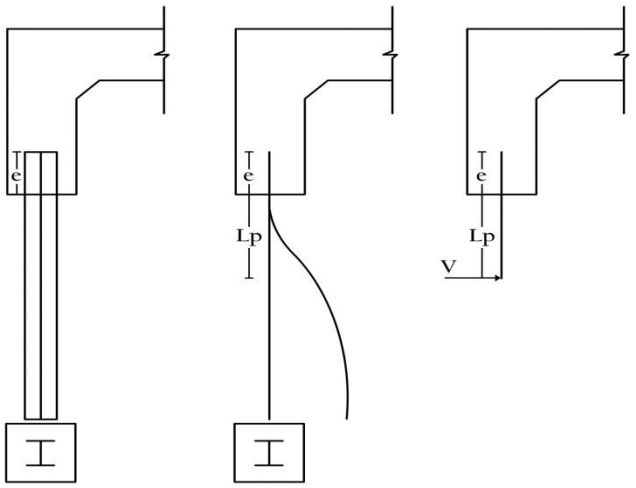

Fig. 4 Point of inflection and embedment depth of pile

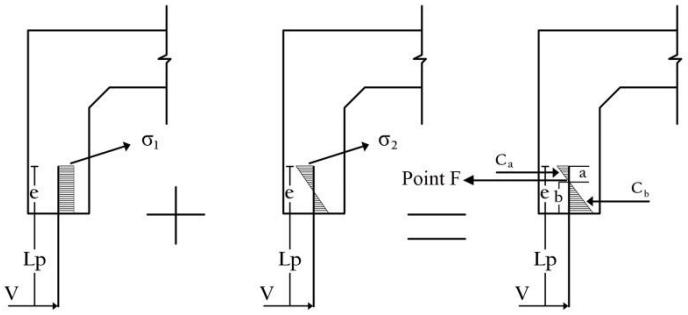

Fig. 5 Bearing stress distribution around pile due to shear and flexure (linear distribution)

• The critical location for concrete failure is assumed to be the front bearing face of the connection and the limiting concrete strength is assumed to be ($f_c^{/}$).

•The confinement effects of surrounding bars around the pile are not considered on the strength of the connection in the present research.

As shown in Fig. 4, *e*, is the embedment length of the pile and (L_p) is distance from point of application of lateral load (inflection point) to concrete surface; so that, the moment is equal to zero at this point on the pile. The length of (L_p) in H section is variable between 3*d* to 5*d*, depending on the soil surrounding the pile (Shama *et al.* 2001). (*V*) is a hypothetical force that is applied at the inflection point and generates bending moment at the connection. The stresses due to the bending and shear for the connection are shown in Fig. 5. According to Figs. 4 and 5, if (C_a) is the force applied to the pile in the front face of the concrete and (C_b) is the force which is applied by the inside and the back face of the concrete. The summation of the forces in the direction of the applied shear force is

$$V + C_a = C_b \tag{4}$$

By writing the moment equation about point F in Fig. 5, Eq. (5) is obtained

$$C_{\mathrm{a}} \times (\frac{2}{3})\mathrm{a} + C_b \times (\frac{2}{3})b = V \times (L_P + b) = M_c \tag{5}$$

In this equation, (a) is the length of stress triangle in the front face of concrete and *b* is the length of stress triangle inside and in the back face of concrete (Fig. 5). (M_c) is the applied moment to the connection. Considering the triangle similarity in stress according diagram according to Fig. 5, Eq. (6) is obtained

$$\frac{b}{\mathrm{a}} = \frac{\sigma_1 + \sigma_2}{\sigma_1 - \sigma_2} \tag{6}$$

If the compressive stress in the front face of concrete is limited to the specified strength of concrete (Burdette *et al*. 1983), it can be written as

$$\sigma_1 + \sigma_2 = f'_c \tag{7}$$

The sum of forces applied by concrete to pile on front and back faces can be determined as

$$C_a = \frac{1}{2} \times b_W \times \mathrm{a} \times (\sigma_2 - \sigma_1) \tag{8}$$

$$C_b = \frac{1}{2} \times b_W \times b \times (\sigma_1 + \sigma_2) \tag{9}$$

According to Fig. 5, the stress due to shear is

$$\sigma_1 = \frac{V}{e \times b_w} \tag{10}$$

Where, *e* is the embedment length of the steel pile. Assuming that (I) is the moment of inertia of the vertical section (a rectangular section in which the length is *e* and the width is b_w). *c* is the distance of neutral axis from the extreme tension or compression fiber. The stress due to bending moment is

$$\sigma_2 = \frac{M_c \times c}{I} = \frac{M_c \times \left(\frac{e}{2}\right)}{(\frac{1}{12}) \times b_w \times e^3} = \frac{6 \times M_c}{b_w \times e^2} \tag{11}$$

When the required embedment length is reached, M_c intends towards to M_p, where M_p is the plastic moment of the pile section. In this study it was assumed that M_c reaches to M_p. Therefore, in the following equations M_c is replaced with M_p.

(C_a) is determined from Eq. (4) and is placed in Eq. (5). Then, by inserting the values obtained from Eqs. (7) through (10) in Eq. (5), Eq. (12) is obtained

$$\frac{1}{3} \times b^2 \times b_w \times f'_c + \frac{1}{3} \times b \times \mathrm{a} \times b_w \times f'_c - \frac{2}{3} \times \frac{M_P \times \mathrm{a}}{(L_P + b)} = M_P \tag{12}$$

Using Eqs. (7), (10) and (11) in Eq. (6), Eq. (13) is obtained.

$$\frac{b}{\mathrm{a}} = \frac{f'_c}{\frac{6 \times M_P}{b_w \times (b + \mathrm{a})^2} - \frac{M_P}{b_w \times (\mathrm{a} + b) \times (L_P + b)}} \tag{13}$$

(a) Formworks

(b) Pouring of fresh concrete

(c) curing

(d) Attaching to solid ground

Fig. 6 Fabrication procedures of abutment-pile connection specimens

By solving the Eqs. (12) and (13) simultaneously, the values of (a) and (b) are determined. The embedment length can be determined using Eq. (14).

$$a + b = e \tag{14}$$

4. Laboratory studies

In order to choose initial values for embedment lengths for tests, the values calculated from Eq. (14) were used. So that, less and longer lengths for specimens were chosen according to the calculated values. This was done to understand the retrofitted and without retrofitting behaviour of specimens. In specimen 1, the embedment length of the pile inside the abutment was used as 23 cm which was a longer than the calculated value (17.48 cm). In the next three specimens (specimens 2 through 4), the embedment length was chosen as 13 cm which was less than the length obtained from Eq. (14). The steps required to fabricate the specimens are shown in Fig. 6. Fig. 7 shows the details of each specimen. These specimens were built to half-scale of the Story

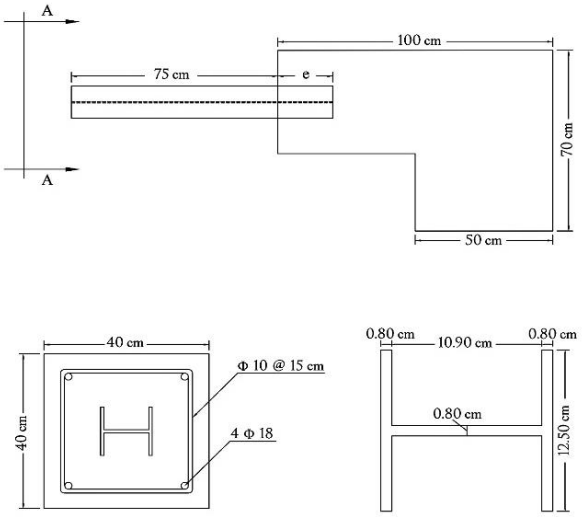

Fig. 7 Details of pile-abutment connection specimens

Table 1 Material properties of abutment concrete

Curing time	Compressive strength (MPa)
Design	25
Curing (28 days)	23.90
At the test time	24.50

County integral bridge (Nilsson *et al*. 2008). The Story County Bridge consists of three spans with an overall length of 201 ft and a skew angle of 15°.

5. Material properties

All of the material properties of the specimens were determined in accordance with ASTM standard test methods. Concrete specifications accordance with ASTM-C39 (2005) and the results from standard tests are given in Table 1. Grade AIII rebar was used for longitudinal and transverse reinforcement. In order to determine the mechanical properties of the steel pile and the stress-strain curve, tensile tests were performed on 3 specimens (Fig. 8). Test specimen dimensions and test specifications were in accordance with ASTM-A370 (2005). The results are given in Table 2.

6. Test method

A static loading was applied to the pile-abutment connection by a hydraulic jack with a capacity of 50 Tons. The applied load and connection of the specimen to the rigid floor of the laboratory are shown in Fig. 9. In order to evaluate the connection behaviour, 3 LVDTs were installed as shown in Fig. 10, to measure displacements. LVDT1 was used to determine the

Fig. 8 Tensile test specimens of pile steels

Table 2 Material properties of H-pile steel

Specimens	Yield strength (MPa)	Tensile strength (MPa)	Elongation (%)
Specimen 1	274	392	34
Specimen 2	277	379	32
Specimen 3	267	377	36
Average	272.66	382.66	34

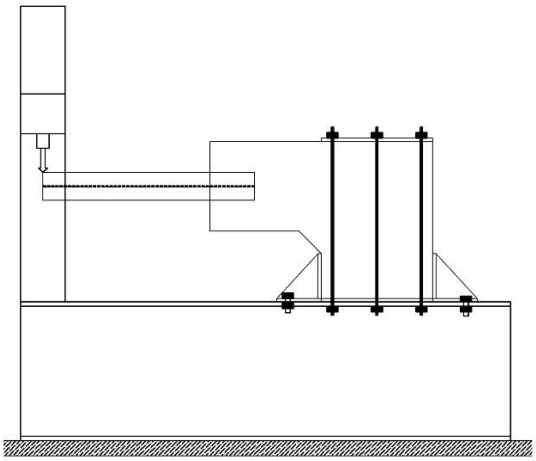

Fig. 9 Set-up of test specimens

displacement of the pile head, while LVDT2 and LVDT3 were used to determine the rotation of the connection. Also strain gauges were installed on different parts of the pile as shown in Fig. 10.

The applied loads, displacements and strains were obtained from the installed data logger. Loading was applied in force control to specimens. The first specimen had an embedment length of 23 cm (determined by Eq. (14)) and the second specimen had an embedment length of 13 cm (less than the length determined by Eq. (14)). The failure mechanisms of both specimens are shown in Fig. 11. The illustrations shown in Fig. 12 help to understand better the crack distribution and propagation. As it can be seen in Fig. 11, failure in specimen 2 is accompanied by the

propagation of upper cracks; and the upper portion of the pile getting pulled out of the concrete. Hence, the pile does not reach fully plastic state at the connection and the connection strength is lower than flexural strength of the pile; whereas in specimen 1 which had adequate embedment length, the pile reaches plastic state at the connection and the connection achieves its maximum strength which is equal to the flexural strength of the pile.

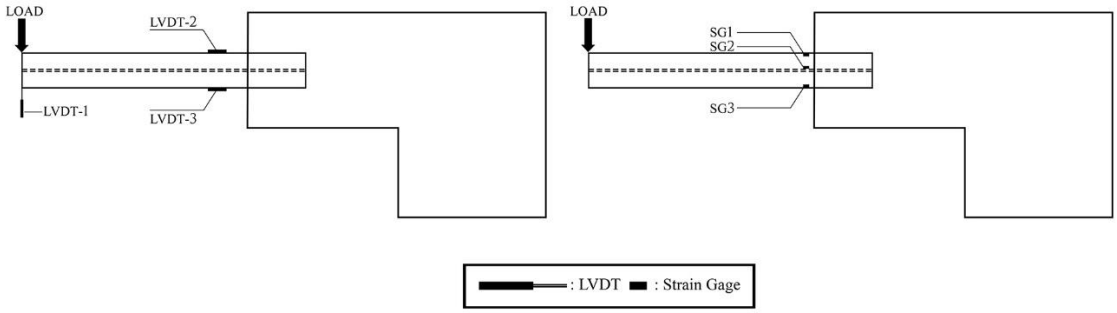

Fig. 10 measurements of test specimens

(a) Specimen 1 (side view)

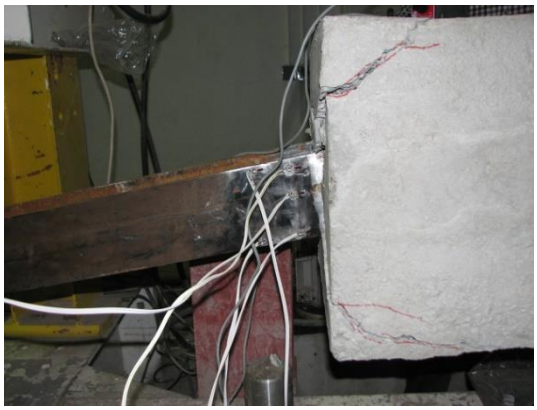

(b) Specimen 2 (side view)

(c) Specimen 1 (front view)

(d) Specimen 2 (front view)

Fig. 11 Cracks and its propagations of specimens and bending of piles

(e) Bending of pile (specimen 1)

(f) Bending of pile (specimen 2)

Fig. 11 Continued

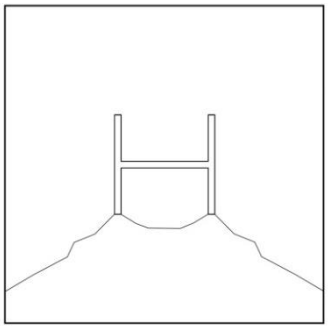

(a) Specimen 1

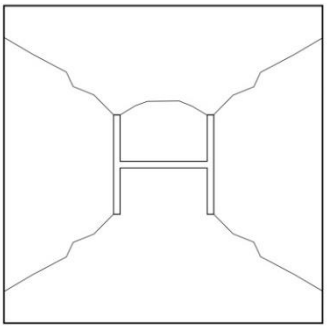

(b) Specimen 2

Fig. 12 Cracks and its propagations of specimens

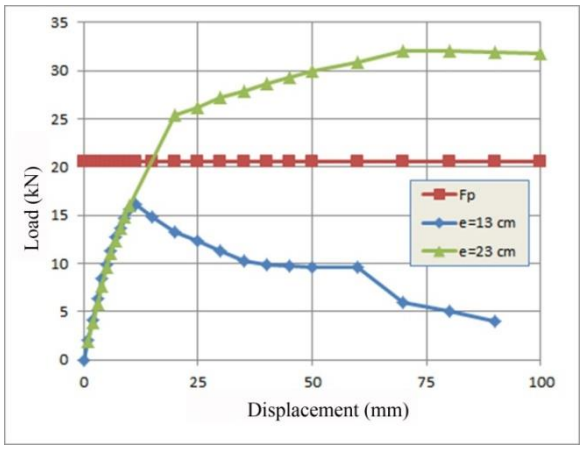

Fig. 13 Load-displacement relationships (LVDT1)

Force-displacement curves determined by LVDT1 for both specimens are shown in Fig. 13. As shown in the figure, the specimen with an embedment length of 13 cm is not able to reach the

target strength, Fp. (Fp is the force that causes the pile to achieve its plastic strength); whereas the specimen 1 with sufficient embedment length has higher strength than Fp and the connection achieves its full plastic strength. Moment-curvature curves for both specimens are shown in Fig. 14. As seen in the figure, the flexural strength of the connection in the specimen 1 has reached the flexural strength of the steel pile, whereas the flexural strength of the connection in the specimen 2 is less than the flexural strength of the steel pile. Ultimate strains at various points on both specimens are given in Table 3. The results from the specimen 2 showed that only the upper portion of the pile yielded and the rest still had linear behaviour. However, the pile at the connection of the specimen 1 reached its yield strength and the connection of the specimen 1 reached the flexural strength of the pile.

7. Retrofitting of connection with CFRP

The loading tests results of specimens 1 and 2 showed that the connection of the specimen 1 with sufficient embedment length (23 cm) provided the required flexural strength; whereas the connection of the specimen 2 with an embedment length of 13 cm did not. Hence, knowing the flexural weakness of the specimen 3 and specimen 4 (due to insufficient embedment length); they were retrofitted with CFRP materials. As shown in Fig. 15, retrofitting with CFRP was carried out based on crack propagation to delay crack initiation. CFRP wraps of type SikaWrap-200C with a width of 13 cm were used. The used specifications of the CFRP are given in Table 4.

In the specimen 3, CFRP were vertically placed on sides of the pile (Fig. 15(a)) and in specimen 4, CFRP were vertically and horizontally attached to sides, top and bottom of the pile

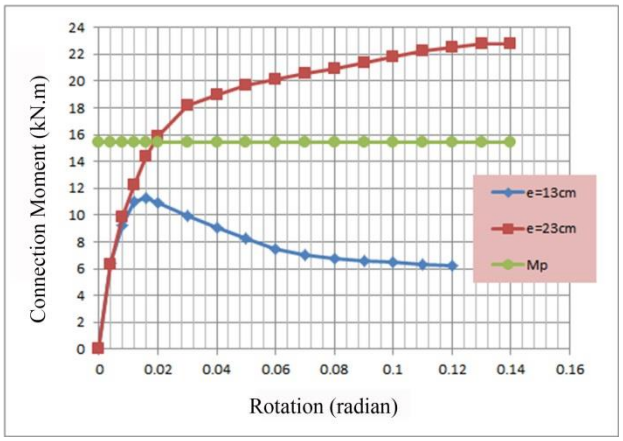

Fig. 14 Moment-rotational angle relationships

Table 3 Ultimate strain of piles

	Specimen1	Specimen2
SG1	0.0014	0.02
SG2	0.0002	0.0013
SG3	0.0006	0.015

Table 4 Material properties of CFRP wraps

Trade mark	Yield strength (MPa)	Young's modulus (GPa)	Thickness of each layer (mm)
Sika Wrap-200c	3900	230	0.11

(a) Attaching of CFRP on the specimen 3

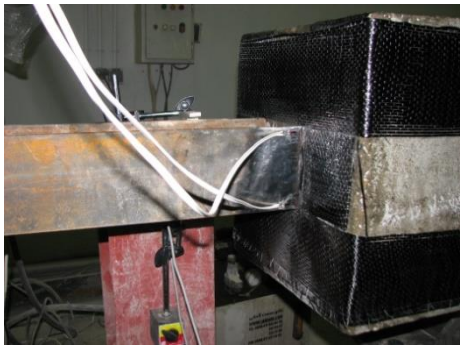

(b) Attaching of CFRP on the specimen 4

(c) Failure mechanism of the specimen 3

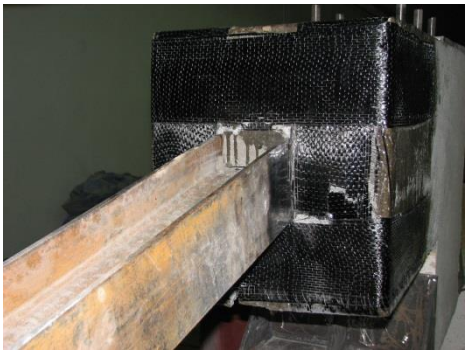

(d) Failure mechanism of the specimen 4

Fig. 15 CFRP reinforcement details and failure mechanisms

(Fig. 15(b)). The failure mechanisms of the retrofitted connections are shown in Fig. 15(c) and Fig. 15(d). First, the specimen 3 was subjected to lateral force. In this specimen, the initiation of 45 degree cracks in the connection was prevented by vertical FRP but vertical cracks were observed. The failure mechanism initiated with failure of the FRP and no de-bonding of FRP from concrete prior to FRP failure was observed. By observing how the failure occurred in the specimen 3, horizontal layers of CFRP were placed to prevent vertical cracks. In this case, due to the adequate strength of the connection, plastic deformation was first observed in the steel pile. The subsequent connection failure was accompanied with failure in vertical FRP. No de-bonding of FRP from concrete - prior to FRP failure - was observed in this case.

The results of loading tests on the retrofitted specimens and their comparison with those of the weak connection are shown in Fig. 16. As it can be seen in Fig. 16, the retrofitting of connection in the specimen 3 (FRP1) has increased the strength of connection by up to 56% and the retrofitting of connection in the specimen 4 (FRP2) has increased the strength of connection by up to 0.86%. In addition, due to plastic deformation of the steel pile, the specimen 4 showed higher ductility than the specimen 3. In both specimens, the strength of the connection was greater than the target strength Fp. Where, Fp is the lateral force that causes the pile to achieve its plastic strength.

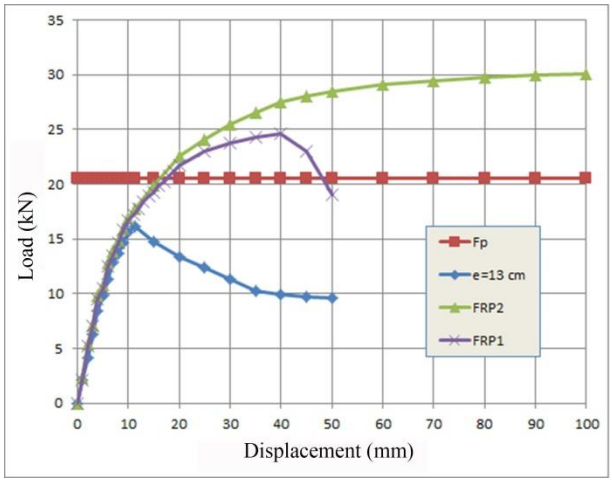

Fig. 16 Load-displacement relationships (LVDT1)

8. Finite element modeling

The finite element models of the specimen 1 (with embedment length equal to 23 cm) and the specimen 4 were created using ATENA software (Červenka 2013) (Fig. 17). The specimens were modelled with fully fixed bases. Solid-CCIsoBrick element was used to model the concrete abutment and the steel pile. Contact-Gap element was used to model the connection between the concrete and steel. Confinement-sensitive plasticity constitutive model (Papanikolaou 2007) was used to model the characteristics of concrete behaviour. This model combines constitutive models for tensile (fracturing) and compressive (plastic) behavior. The fracture model is based on the classical orthotropic smeared crack formulation and crack band model. It employs Rankine failure criterion, exponential softening, and it can be used as rotated or fixed crack model. The hardening/softening plasticity model is based on (Menétrey-Willam 1995) failure surface. Materials used in this model can handle the increased deformation capacity of concrete under triaxial compression. It is suitable for problems including confinement effects such as confined reinforced concrete members. To model the behaviour of the steel, the Von Mises model with strain hardening was used. Connection between concrete and steel was modelled using the Coulomb model of friction. The coefficient of friction between concrete and steel was taken as 0.4. In different references - such as French code - values close to 0.4 are used for the coefficient of friction (Raous *et al*. 2009). Since no de-bonding of CFRP from concrete was observed in tests, bar element with the same area and properties of CFRP was used to model CFRP elements. Also, linear behaviour with rupture point was chosen.

Finite element models of specimens 1 and 4 are shown in Fig. 17(a) and Fig.17 (b) respectively. The force-displacement curves for specimens 1 and 4 (at LVDT1) are shown for analytical and experimental cases in Fig. 18. The comparison of curves showed that the displacements determined by FE analysis compared well with the experimental results. In small displacements within the linear range, FE analysis resulted in greater values than experimental data. This difference in stiffness and strength can be justified by the fact that fully fixed boundary conditions were applied in the finite element model; whereas these conditions are not possible to implement in practice.

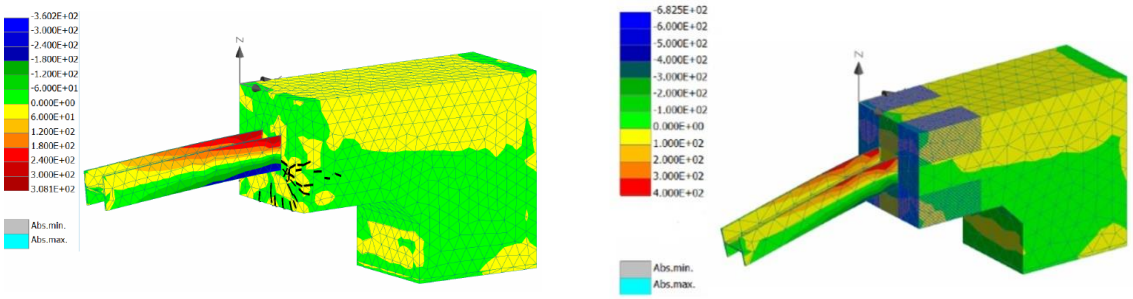

(a) Specimen 1 (b) Specimen 4

Fig. 17 Finite element models of specimens

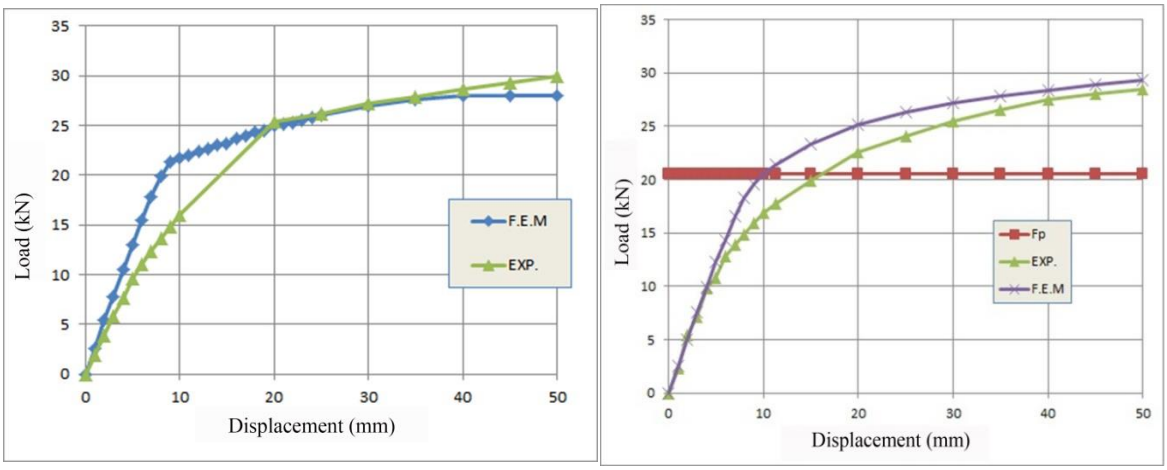

(a) Specimen 1 (b) Specimen 4

Fig. 18 Comparisons of test results with FE analysis results

9. Conclusions

The main object of the present research was experimental investigation on steel pile connection to integral bridge abutment retrofitting. Retrofitting details using CFRP materials was provided to strengthen weak connections (inadequate embedment length). To calculate the pile embedment length based on plastic flexural strength, a theoretical method was proposed. The calculated values obtained from the proposed method were used to choose the embedment lengths.

Four connection specimens with a half scale were tested. Also, finite element analyses were performed and the following results were obtained:

- By increasing of embedment length from 13 cm ($\frac{e}{b_w}=1.04$) to 23 cm ($\frac{e}{b_w}=1.84$) the strength of connection was increased up to 100%.
- The flexural strength of specimen 1 (with the embedment length of e=23 cm) was reached to the pile flexural strength.
- The connection retrofitting of specimens 3 and 4 caused the increase of strength up to 56%

and 86%, respectively.

• To increase the strength and ductility of the connection, the use of vertical and horizontal CFRP (Details for the specimen 4) on all sides of the steel pile is recommended.

• FE modeling using ATENA software predicted the strength of the connection to a reasonable extent.

References

ACI 318-14/ACI 318R-14 (2014), Building Code Requirements for Reinforced Concrete and Commentary, American Concrete Institute.

Arsoy, S. (2000), "Experimental and analytical investigations of piles and abutments of integral", Doctoral Thesis, Virginia Polytechnic Institute and State University, Blackburg.

ASTM A370 (2005), Standard Test Methods and Definitions for Mechanical Testing of Steel Products, American society for testing and materials.

ASTM C39 (2005), Standard Test Method for Compressive Strength of Cylindrical Concrete Specimens, American Society for Testing and Materials.

Burdette, E.G., Jones, W.D. and Fricke, K.E. (1983), "Concrete bearing capacity around large inserts", ASCE Journal of Structural Engineering, **109**(6), 1375-86.

Burke, Jr. M. P. (2009), *Integral and Semi-Integral Bridges*, John Wiley & Sons, Oxford.

Červenka, V. and Červenka, J. (2013), User's Manual for ATENA 3D Version 5.0.0.

Dicleli, M. and Albhaisi, S.M. (2003), "Maximum length of integral bridges supported on steel H-piles driven in sand", *Eng. Struct.*, **25**, 1491-504.

Dicleli, M. and Albhaisi, S.M. (2004), "Performance of abutment-backfill system under thermal variations in integral bridges built on clay", *Eng. Struct.*, **26**, 949-62.

Haj-Najib, R. (2002), "Integral abutment bridges with skew angles", Ph.D. Dissertation, Univ. of Maryland, College Park, MD.

Harries, K.A. and Petrou, M.F. (2001), "Behavior of precast, pre-stressed concrete pile to cast-in-place cap connections", *PCI J.*, **46**(4), 82-92.

Jin, H.A., Ji, H.Y., Jong, H.K. and Sang, H.K. (2011), "Evaluation on the behavior of abutment-pile connection in integral abutment bridge", *J. Constr. Steel Res.*, **67**, 1134-1148.

Kappes, L., Berry, M., Stephens, J. and McKittrick, L. (2012), "Concrete filled steel tube piles to concrete pile-cap connections", *Struct. Congress*, doi: 10.1061/9780784412367.052.

Kotsoglou, A.N. and Pantazopoulou, S.J. (2009), "Assessment and modeling of embankment participation in the seismic response of integral abutment bridges", *Bull Earthq. Eng.*, **7**, 343-361.

Kunin, J. and Alampulli, S. (2000), "Integral abutment bridges current practice in United States and Canada", *J. Perform. Constr. Facil.*, ASCE, **14**(3), 104-11.

Menetrey, P. and Willam, K.J. (1995), "Triaxial failure criterion for concrete and its generalization", *ACI Struct. J.*, **92**(3), 311-318.

New York state department of transportation (2007), "Integral abutment bridges: comparison of current practice between European countries and the United States of America", Special Report, Transportation Research and Development Bureau.

Nilsson, M. (2008), "Evaluation of in-situ measurements of composite bridge with integral abutments", Thesis, Luleå University of Technology Department of Civil, Mining and Environmental Engineering Division of Structural Engineering.

Pam, H.J. and Park, R. (1990), "Simulated seismic load tests on pre-stressed concrete piles and pile-pile cap connections", *PCI J.*, **35**(6), 42-61.

Papanikolaou, V.K. and Kappos, A.J. (2007), "Confinement-sensitive plasticity constitutive model for concrete in triaxial compression", *Int. J. Solid. Struct.*, **44**(21), 7021-7048.

Park, Y.H. and Nam, M.S. (2007), "Behavior of earth pressure and movements on integral abutments", *J.*

KSCE, **26**, 949-62.
Park, Y.H., Jung, G.J. and Kim, S.H. (2000), "Axial response of impact-driven H piles using integral abutment bridge", *J. KSCE,* **20**(3C), 281-90.
Park, Y.H., Jung, H.S., Lee, Y.S. and Jung, G.J. (2001), "Lateral behavior of impact-driven H piles used in integral abutment bridge", *J. KSCE*, **21**(3C), 207-23.
Petursson, H. and Collin, P. (2002), *IABSE Symposium Melbourne, Composite Bridges with Integral Abutments minimizing Lifetime Costs*, Melbourne.
Raous, M. and Karray, M.A. (2009), "Model coupling friction and adhesion for steel concrete interfaces", *Int. J. Comput. Appl. Tech. Intersci.,* **34** (1), 42-51.
Shama, A.A. and Mander, J.B. (2001), "Seismic performance and retrofit of steel pile to concrete cap connections", *ACI Struct. J.*, **99**(1), 185-192.
Sherafati, A. and Azizinamini, A. (2015), "Flexible pile head in jointless bridges: experimental investigation", *J. Bridge Eng*., **20**(4), 04014071.
Stephens, J. and Mc.Kittrick, L. (2005), "Performance of steel pipe pile-to-concrete bent cap connections subject to seismic or high transverse loading: phase II", Report No.FHWA/MT-05-001/8144.
Steunenberg, M., Sexsmith, R. and Stiemer, S. (1998), "Seismic behavior of steel pile to precast concrete cap beam connections", *J. Bridge Eng.*, **3**(4), 177-185.
Xiao, Y. (2003), "Experimental studies on precast pre-stressed concrete pile to CIP concrete pile-cap connections", *PCI J*., **48**(6), 82-91.
Xiao, Y., Wu, H, Yaprak, T.T., Martin, G.R. and Mander, J.B. (2006), "Experimental Studies on Seismic Behavior of Steel Pile-to-Pile-Cap Connections", *J. Bridge Eng*., ASCE, **11**(2), 151-159.

CC

Notations

a	the length of stress triangle in the front face of concrete
b	the length of stress triangle inside and in the back face of concrete
b_w	the width of steel pile
c	the distance of neutral axis from the extreme tension or compression fiber
C	the assumed concrete forces resisting the moment
C_a	the force applied to the pile in the front face of the concrete
C_b	the force which is applied by the inside and the back face of the concrete
e	the embedment length of the pile
$f_c^{/}$	concrete compressive strength
I	the moment of inertia of the concrete section (a rectangular section in which length is e and the width is b_w)
L_p	distance from point of application of lateral load to concrete surface
M_c	moment capacity of connection
M_p	moment capacity of steel pile section
V	horizontal applied load on pile
β_1	factor relating depth of equivalent rectangular compressive stress block to depth of neutral axis
σ_1	compressive stress in the front face of concrete due to shear
σ_2	compressive stress in the front face of concrete due to bending